

Article

# Luminescence and Electron–Hole-Trapping Centers in $\alpha$ - $Ca_2P_2O_7$ – $Mn$

Turlybek N. Nurakhmetov <sup>1</sup>, Temirulan T. Alibay <sup>1</sup>, Keleshek B. Zhangylyssov <sup>1</sup>, Aibek S. Nurpeissov <sup>1,\*</sup>, Sapargali Pazylybek <sup>2</sup>, Diana Griesiute <sup>2</sup>, Aleksej Zarkov <sup>2</sup> and Aivaras Kareiva <sup>2</sup>

<sup>1</sup> L.N. Gumilyov Eurasian National University, st. Satpaev-2, Astana Z01A3D7, Kazakhstan; keleshek92@yandex.ru (K.B.Z.)

<sup>2</sup> Institute of Chemistry, Faculty of Chemistry and Geosciences, Vilnius University, Naugarduko 24, LT-03225 Vilnius, Lithuania

\* Correspondence: lord\_sukre@mail.ru

**Abstract:** The mechanisms of formation of induced intrinsic and impurity radiative states, which consist of intrinsic and impurity electron–hole-trapping center states in irradiated  $Ca_2P_2O_7$ – $Mn$  and  $Ca_2P_2O_7$  phosphates, were investigated using thermoactivation and vacuum-ultraviolet spectroscopy methods. These centers are excited at photon energies of 4.0 eV and 4.5 eV, which are within the matrix’s transparency region. New radiative-induced states at 3.06 eV and 2.92 eV are demonstrated to be generated upon the excitation of anions by photons with energies of 5.0 and 5.64 eV. This process is due to charge transfer from the ion to the impurities, specifically  $Mn^{2+}(O^{2-} - Mn^{2+})$  and the neighboring ion  $O^{2-} - (P_2O_7)^{4-}$ . Furthermore, upon the excitation of matrix anions with photon energies exceeding the band gap (8.0–8.25 eV), electron-trapping by impurities such as  $Mn^{2+}$  and  $(P_2O_7)^{4-}$  ions results.

**Keywords:** electrons and holes; trapping center; luminescence; XRD; SEM; emission spectra; excitation spectra



**Citation:** Nurakhmetov, T.N.; Alibay, T.T.; Zhangylyssov, K.B.; Nurpeissov, A.S.; Pazylybek, S.; Griesiute, D.; Zarkov, A.; Kareiva, A. Luminescence and Electron–Hole-Trapping Centers in  $\alpha$ - $Ca_2P_2O_7$ – $Mn$ . *Crystals* **2024**, *14*, 406. <https://doi.org/10.3390/cryst14050406>

Academic Editor: Bertrand Poumellec

Received: 1 March 2024

Revised: 29 March 2024

Accepted: 23 April 2024

Published: 26 April 2024



**Copyright:** © 2024 by the authors. Licensee MDPI, Basel, Switzerland. This article is an open access article distributed under the terms and conditions of the Creative Commons Attribution (CC BY) license (<https://creativecommons.org/licenses/by/4.0/>).

## 1. Introduction

Calcium phosphates constitute a diverse family of materials that find widespread use in a variety of fields, including as medicine for bone regeneration, catalysis, sensor technology, and as foundational matrices for the development of optical materials. In the study of these materials’ optical properties, special emphasis is placed on examining the luminescent characteristics of doped phosphates. These luminescent properties are pivotal in the creation of white light sources, which are achieved by coating blue near-ultraviolet-emitting LED chips with phosphors [1]. Furthermore, the enduring phosphorescence and thermoluminescence exhibited by phosphates hold promise for a range of applications across the energy sector, lighting, and optical visualization in the red and infrared spectral ranges [2].

To advance the applications mentioned above, numerous studies have been conducted on the luminescent properties of phosphates. For instance, the research conducted by authors [3] demonstrated the luminescent characteristics of  $KSrPO_4$  activated by  $Eu^{3+}$  following irradiation with synchrotron radiation. It was revealed that  $Eu^{2+}$  ions are formed in the excited state as a result of charge transfer from the matrix to the impurities ( $O^{2-} - Eu^{3+}$ ). The charge transfer from  $O^{2-}$  to  $Eu^{3+}$  requires an energy of 4.6 eV. During the relaxation process from the excited state back to the ground state, recombination emission occurs at 2.9 eV, corresponding to the  $4f^65d - 4f^7$  transition. Additionally, the energy gap from the excited electronic state of  $Eu^{2+}$  to the bottom of the conduction band is estimated to be 0.4 eV.

The nature of impurity emission centers in phosphates activated by  $Mn^{2+}$  ions was the focus of investigations by the authors of [3,4]. In  $Ca_2P_2O_7$ – $Mn$ , it was discovered that

broad emission bands at 2.17 eV, 2.08 eV, and 2.14 eV are excited by several bands at 2.48 eV, 3.1 eV, 2.95 eV, and 3.44–3.65 eV. According to the hypothesis presented by the authors in [4], these excitation spectra are indicative of forbidden intra-center transitions of  $Mn^{2+}$  ions situated at the cationic sites of the crystal lattice. Further, authors in [3] identified that emission at 1.93 eV, which is not only excited by intracenter bands but also efficiently by UV emission at 5.9 eV, can be attributed to charge transfer from the matrix,  $Ca_5Mn(PO_4)_7$ , to the  $Mn^{2+}$  impurities ( $O^{2-} - Mn^{2+}$ ). Additionally, the observation of thermoluminescence at 240 K and between 400 and 477 K, along with phosphorescence, is linked to the creation of trap centers during X-ray excitation.

The formation of electron–hole-trapping centers in phosphates was observed during photon irradiation, with energies surpassing the band gap, leading to the creation of free electron–hole pairs. In the research conducted by authors [5], thermoluminescence (TL) was studied in  $YPO_4$  doped with  $Ce^{3+}$  and  $Ln^{3+}$  (where  $Ln$  represents  $Nd^{3+}$ ,  $Er^{3+}$ ,  $Ho^{3+}$ ,  $Dy^{3+}$ ). During the irradiation of  $YPO_4 : Ce^{3+}, Ln^{3+}, Ln^{2+}$  electron-trapping centers are formed by the trapping of free electrons. Simultaneously, the trapping of holes by the  $Ln^{3+}$  ground state leads to the formation of  $Ln^{4+}$  hole trapping centers. TL is observed because of the recombination decay of these electron–hole-trapping centers.

Phosphors doped with  $Eu^{2+}$  impurities are utilized as sources of green radiation, which is instrumental in exciting hole-trapping centers, thereby generating stable red and infrared radiation. The photoluminescence, radioluminescence, and phosphorescence properties of these phosphors, when doped with rare earth ions, have been extensively studied by the authors in references [6–16].

In reviews and summary articles [17–19], the optical properties of non-rare-earth ions  $Mn^{4+}$  and  $Mn^{2+}$  have been investigated by the authors. Their properties were compared with the known properties of  $Eu^{2+}$  light-emitting diodes, which emit red light in various materials. It has been demonstrated that from an economic standpoint,  $Mn^{4+}$  ions, not being rare-earth ions, surpass  $Eu^{2+}$  ions in terms of red-light intensity. The main comparative properties of  $Mn^{4+}$  and  $Eu^{2+}$  ions in various host materials have been considered. Spectral differences in emission between  $Mn^{4+}$  and  $Eu^{2+}$  activator ions have been demonstrated, which can provide green and orange-red emissions depending on their practical application.

In the studies by authors [20,21], the mechanisms for the accumulation of intrinsic and impurity electron–hole-trapping centers were explored in both pure and  $Mn^{2+}$ -activated  $CaSO_4$  and  $BaSO_4$ . It was demonstrated that intrinsic  $SO_4^{3-} - SO_4^-$  and impurity  $Mn^{2+} - SO_4^-$  trapping centers form as a result of free electrons localizing on the  $SO_4^{2-}$  anion and  $Mn^{2+}$  impurities, through the reactions  $SO_4^{2-} + e^- \rightarrow SO_4^{3-}$  and  $Mn^{2+} + e^- \rightarrow Mn^{+}$ .

From a brief review of the literature, several conclusions can be drawn: During the irradiation of excited anion complexes, impurity electron-trapping centers form below the conduction band; when free electrons and holes localize on rare-earth ions, electron- and hole-trapping centers are generated, whose recombination leads to thermoluminescence (TL) and phosphorescence.

This work will discuss the mechanisms of the formation of electron- and hole-trapping centers upon the excitation of the  $Ca_2P_2O_7 - Mn$  phosphor across a broad spectral (from 4 eV to 12 eV) and temperature range (15–300 K). By analyzing the excitation spectra of impurity emission from  $Mn^{2+}$  and the newly created recombination or tunneling emissions comprising electron–hole trapping centers, the study investigates the relaxation processes that facilitate energy transfer to impurities.

## 2. Objects and Research Methods

Undoped and Mn-doped  $Ca_2P_2O_7$  powders were synthesized using the wet co-precipitation method, as described in [4,7]. The Mn substitution rate was set at 1 mol.% relative to  $Ca^{2+}$ . The obtained precipitates were annealed at 1200 °C, with a heating rate of 5 °C/min and a holding time of 10 min.

### Characterization

X-ray diffraction analysis (XRD) of the powders was carried out using Ni-filtered Cu-K $\alpha$  radiation on a Rigaku MiniFlex II diffractometer, operating in the Bragg–Brentano ( $\theta/2\theta$ ) geometry. Data were collected over a  $2\theta$  range from 10 to 60°, with a step size of 0.02° and a scanning speed of 1°/min.

The morphology of the synthesized products was examined using a Hitachi SU-70 (Tokyo, Japan) field emission scanning electron microscope (FE-SEM).

Measurements of emission and excitation spectra in the spectral range from 6.2 eV to 12.4 eV (100–200 nm) were carried out using a vacuum monochromator assembled according to the Seiya–Namioka scheme with a recording monochromator Solar M-266 (Solar LS, Minsk, Belarus) and a PMT detector Hamamatsu H11890-01 (Hamamatsu Photonics, Shizuoka Pref, Japan). A hydrogen lamp is used for excitation in the VUV range of the spectrum. Cooling up to 15 K is provided by a cryostat with helium cooling equipment of a closed cycle.

To measure emission spectra in the range of 1.5–6.2 eV, a Solar SM 2203 (Solar LS, Minsk, Belarus) spectrofluorometer was used. Low-temperature studies (77 K) using a cryostat with a vacuum of 10<sup>−4</sup> Pa cooling were carried out using liquid nitrogen.

The samples were irradiated using a BSV-23 X-ray tube with a copper anode, operating at a tube current of 10 mA and a voltage of 40 kV. The energy range of the X-ray photons was between 10 and 15 keV, and a 150 W xenon lamp XBO (OSRAM GmbH, Garching, Germany) with a photon energy of 1.5–6.2 eV (200–830 nm) was utilized.

### 3. Experimental Results

In order to determine the nature of intrinsic, impurity, and recombination emissions at trapping centers in  $Ca_2P_2O_7$  and  $Ca_2P_2O_7 - Mn$  phosphors, excitation, and emission spectra were studied upon excitation by ultraviolet and X-ray radiation over a wide temperature range from 15 K to 300 K.

The crystallinity and purity of the synthesized powders were assessed using X-ray diffraction analysis. The X-ray diffraction pattern of the  $Ca_2P_2O_7$  sample doped with  $Mn$ , after annealing at 1200 °C, is depicted in Figure 1. The diffraction peaks closely match the standard pattern for  $\alpha$ - $Ca_2P_2O_7$  (PDF #073-0440), confirming the successful formation of the target material. A minor presence of the adjacent phase,  $\alpha$ - $Ca_3(PO_4)_2$ , was also observed, likely resulting from the evaporation of phosphate particles during the process.

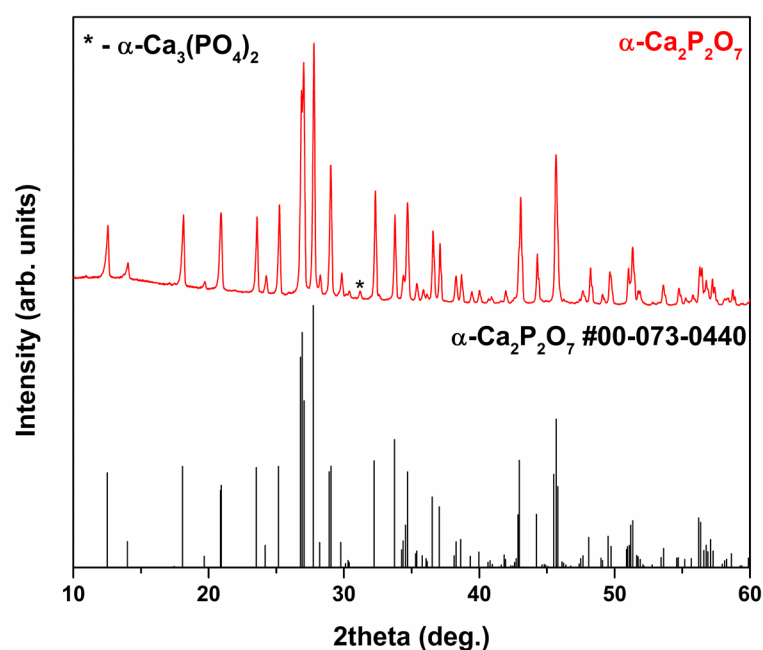
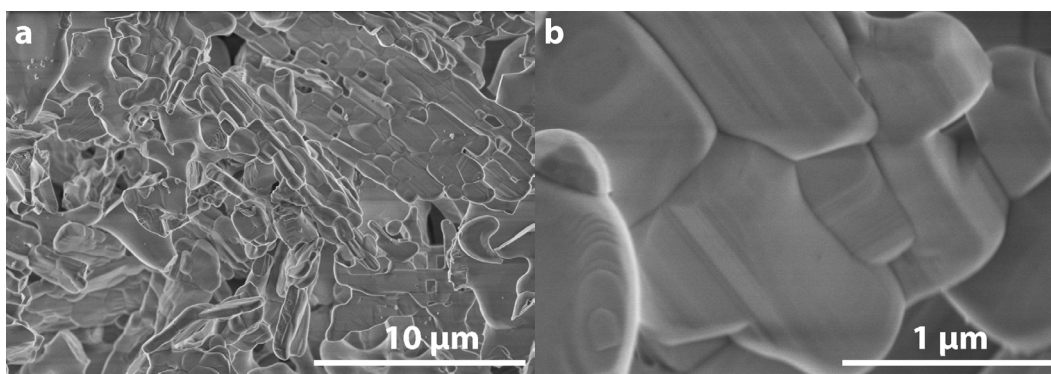


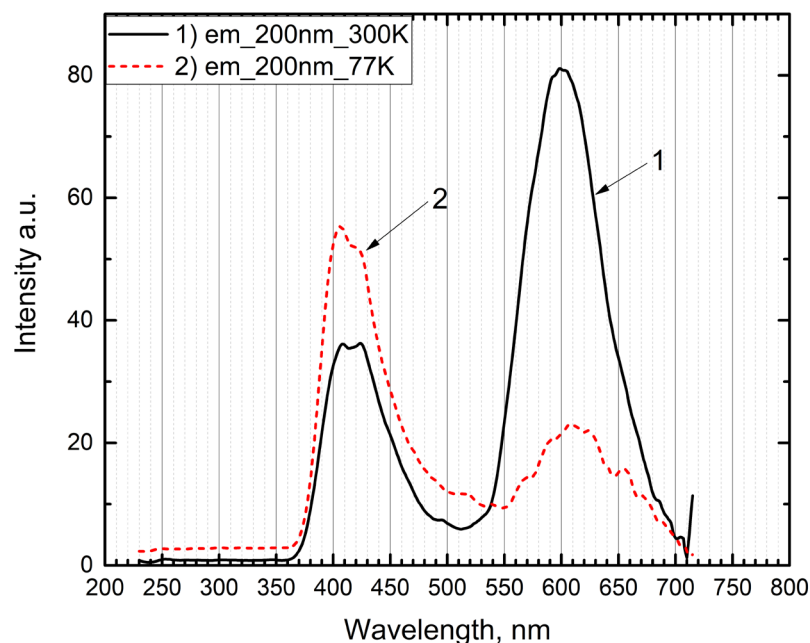
Figure 1. X-ray diffraction pattern of  $\alpha$ - $Ca_2P_2O_7$  :  $Mn$  powder alongside the standard sample.

The morphological characteristics of the synthesized powders were examined through scanning electron microscopy (SEM). Representative SEM images of the Mn-doped  $Ca_2P_2O_7$  sample, displayed in Figure 2, reveal that the powders are composed of a mix of plate-like and irregularly shaped particles. Notably, the plate-like particles exhibit grains ranging in size from micrometers to sub-micrometers.



**Figure 2.** SEM micrographs of  $Ca_2P_2O_7 : Mn$  powder. (a) general view at  $10 \mu m$ ; (b) at magnifications up to  $1 \mu m$ .

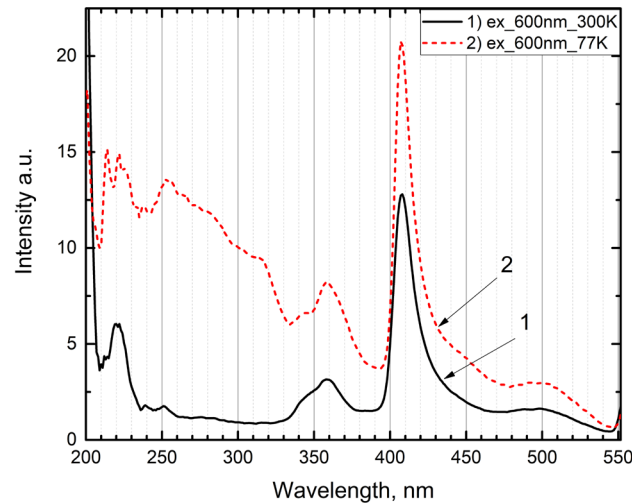
In Figure 3, the emission spectra of the  $Ca_2P_2O_7 - Mn$  phosphor, upon irradiation with 6.2 eV photons at 300 K, is depicted as curve 1. Additionally, the emission spectra measured at 77 K in a cryostat, following excitation with 6.2 eV (200 nm) photons, are shown as curve 2. The analysis of Figure 3 reveals that at 300 K, there is an intracenter emission band at 2.06 eV (602 nm), attributed to the  $Mn^{2+}$  ion within the phosphor (curve 1), alongside the emergence of new emission bands at 3.06 eV (405 nm) and 2.92 eV (425 nm) (curve 1). Notably, at 77 K, the  $Mn^{2+}$  emission band markedly diminishes, whereas the intensity of the newly observed emission bands at 3.06 eV (405 nm) and 2.92 eV (405 nm) experiences a 1.5-fold increase.



**Figure 3.** Emission spectra of the  $Ca_2P_2O_7 - Mn$  phosphor upon excitation with 6.2 eV (200 nm) photons (1—at 300 K, 2—at 77 K).

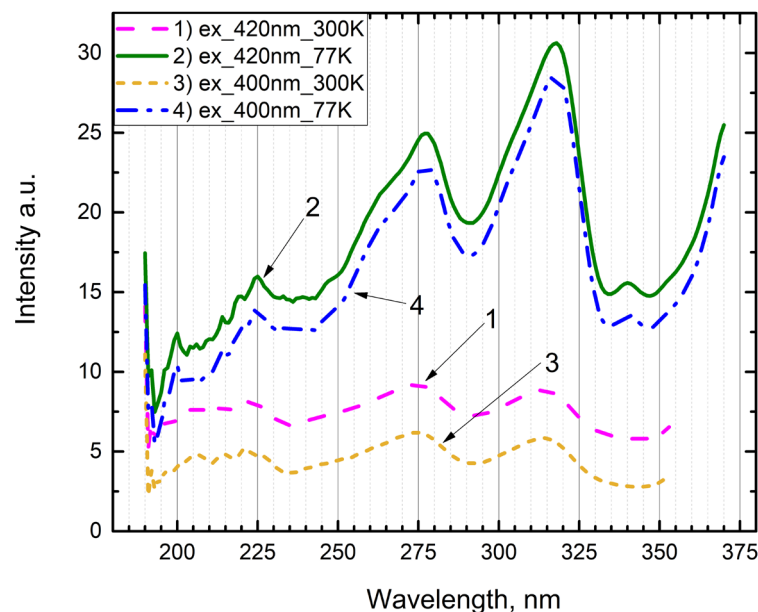
In Figure 4, the excitation spectrum for the main intracenter emission of  $Mn^{2+}$  at 2.06 eV (602 nm), 300 K (curve 1), and 77 K (curve 2) is presented. The analysis of the graph

indicates that at 77 K, the emission band is excited at discrete energies of approximately 2.5 eV (496 nm), 3.0 eV (413 nm), 3.5 eV (354 nm), 4.0 eV (310 nm), 4.5 eV (275 nm), and within the range of 6.2 to 5.0 eV. Conversely, at 300 K, these emission bands also occur but exhibit lower intensity, particularly within the narrower range of 4.0 eV (310 nm) to 4.5 eV (275 nm).



**Figure 4.** Excitation spectra of the intracenter emission for the 2.06 eV (602 nm) band, irradiated  $Ca_2P_2O_7 - Mn$  (1—at 300 K, 2—at 77 K).

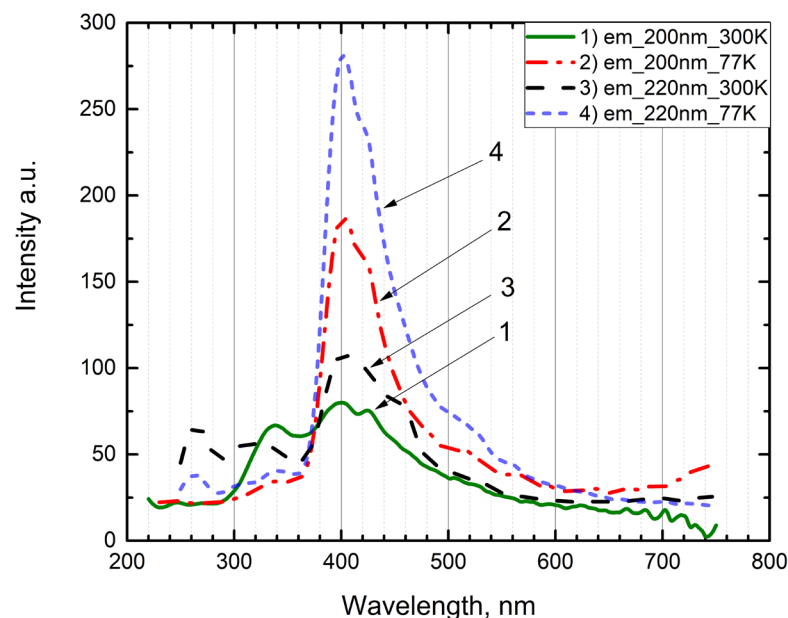
In Figure 5, the excitation spectra for the newly identified bands at 3.06 eV (405 nm) and 2.92 eV (425 nm), following pre-irradiation of the phosphor at 6.2 eV (200 nm), are displayed at both 300 K and 77 K. Excitation bands are identified within the ranges of 3.94–4.0 eV (310–314 nm), 4.5–4.6 eV (269–275 nm), and broadly from 6.2 eV (200 nm) to 5.5 eV (225 nm). Notably, these bands are prominently observed at 77 K, indicating a stronger response to excitation at this lower temperature. Conversely, at 300 K, these same bands manifest as weak excitation bands, suggesting a diminished excitation efficiency at higher temperatures.



**Figure 5.** Excitation spectra of the pre-irradiated phosphor: 1—for the emission band at 2.92 eV (425 nm) at 300 K; 2—for the emission band at 2.92 eV (425 nm) at 77 K; 3—for the emission band at 3.06 eV (405 nm) at 300 K; 4—for the emission band at 3.06 eV (405 nm) at 77 K.

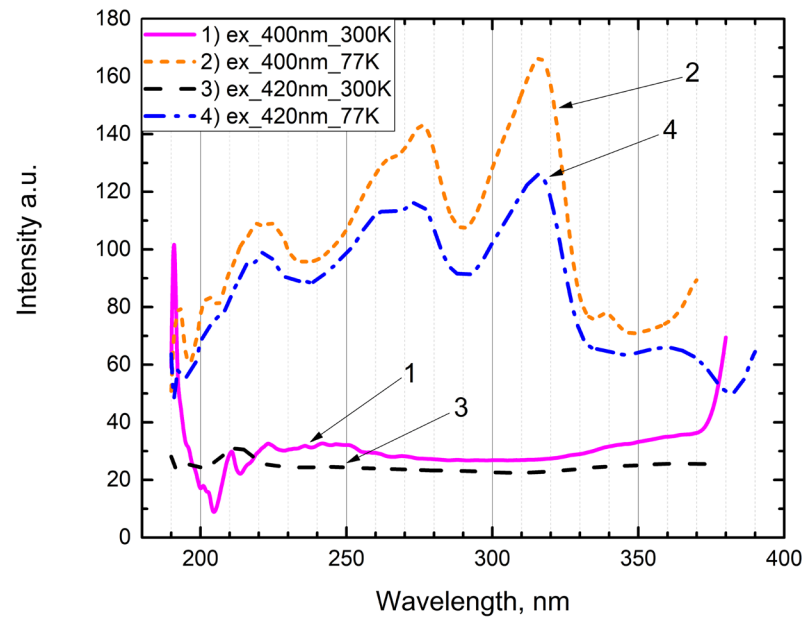
When measuring the excitation spectra for the intracenter emission of the  $Mn^{2+}$  ion at 2.06 eV (602 nm), emission bands similar to those identified by authors in [2] were observed at 2.5 eV (496 nm), 3.1 eV (400 nm), 3.0 eV (413 nm), and between 3.5 eV (354 nm) and 3.6 eV (344 nm). Additionally, alongside the main intracenter emission at 2.06 eV (602 nm) for  $Mn^{2+}$ , the excitation spectrum revealed bands for the newly identified emissions at 3.06 eV (405 nm) and 2.92 eV (419 nm), specifically within the ranges of 3.94–4.0 eV (310–314 nm) and 4.5–4.6 eV (269–275 nm). Furthermore, excitation bands at 5.0 eV (248 nm) and 5.64 eV (220 nm) were also detected. Consequently, these newly emerged emission bands are excited by photon energies of 3.94–4.0 eV (310–314 nm), 4.5–4.6 eV (269–275 nm), 5.0 eV (248 nm), and 5.64 eV (220 nm).

Similar experiments were carried out using pure  $Ca_2P_2O_7$  phosphor. The emission spectrum of this phosphor, when irradiated with photons at energies of 6.2 eV (200 nm) (curves 1 and 2) and 5.64 eV (220 nm) (curves 3 and 4) at temperatures of 77 K and 300 K, is depicted in Figure 6. It is observed that emission bands at 2.92 eV (425 nm) and 3.06 eV (344 nm) appear at both 77 K and 300 K, mirroring those in the  $Ca_2P_2O_7 - Mn$  phosphor.



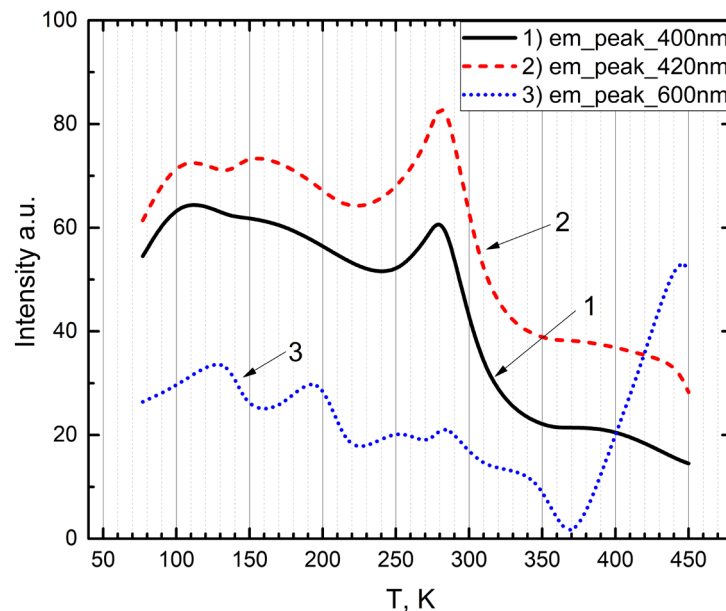
**Figure 6.** Emission spectrum of the phosphor  $Ca_2P_2O_7$  when excited by photons at 6.2 eV (200 nm) (1—at 300 K, 2—at 77 K) and when excited by photons at 5.64 eV (220 nm) (3—at 300 K, 4—at 77 K).

Figure 7 presents the excitation spectra of the pre-irradiated  $Ca_2P_2O_7$  phosphor with UV photons at an energy of 6.2 eV (200 nm) for the recombination emission bands at 2.92 eV (292 nm) (curves 1 and 2) and 3.06 eV (405 nm) (curves 3 and 4), at 300 K and 77 K respectively. In alignment with observations from the  $Ca_2P_2O_7 - Mn$  phosphor, excitation bands are identified at 3.94–4.0 eV (310–314 nm) and 4.5–4.6 eV (269–275 nm), along with a band at 5.64 eV (220 nm). Additionally, in pure phosphates, emissions at 2.92 eV are also excited by photon energies of 4.0 eV (310 nm) and within the range of 4.45–4.6 eV (269–278 nm), occurring within the matrix's transparency region.



**Figure 7.** Excitation spectra of pre-irradiated phosphor: for the emission band at 2.95 eV (420 nm): 1—at 300 K; 2—at 77 K; for the emission band at 3.1 eV (400 nm): 3—at 300 K; 4—at 77 K.

Figure 8 illustrates the temperature-dependent behavior of emission intensity for bands at 2.95 eV (420 nm) (curve 1), 3.1 eV (400 nm) (curve 2), and 2.06 eV (602 nm) (curve 3). The data reveal that the intensity of the recombination emissions at 2.95 eV and 3.1 eV shows a gradual decline starting from 77 K. Moreover, it is observed that the intensity of the intracenter emission associated with the  $Mn^{2+}$  impurity at 2.06 eV (602 nm) decreases in a monotonic fashion until reaching 350 K, beyond which it experiences a sharp increase up to 450 K.



**Figure 8.** Temperature dependence of emission intensity at 1—at 2.95 eV (420 nm); 2— at 3.1 eV (400 nm); and 3— at 2.06 eV (600 nm).

Figure 9 illustrates the TL curve of  $Ca_2P_2O_7 - Mn$ . In the  $Ca_2P_2O_7 - Mn$  phosphor irradiated with X-rays at 77 K, TL peaks appear at 200–270 K, 350 K, and 400–440 K. TL

peaks appear in the temperature range where the intensity of the emission 2.92 eV (425 nm) and 3.06 eV of the combined radiative state of the phosphor  $Ca_2P_2O_7 - Mn$  changes.

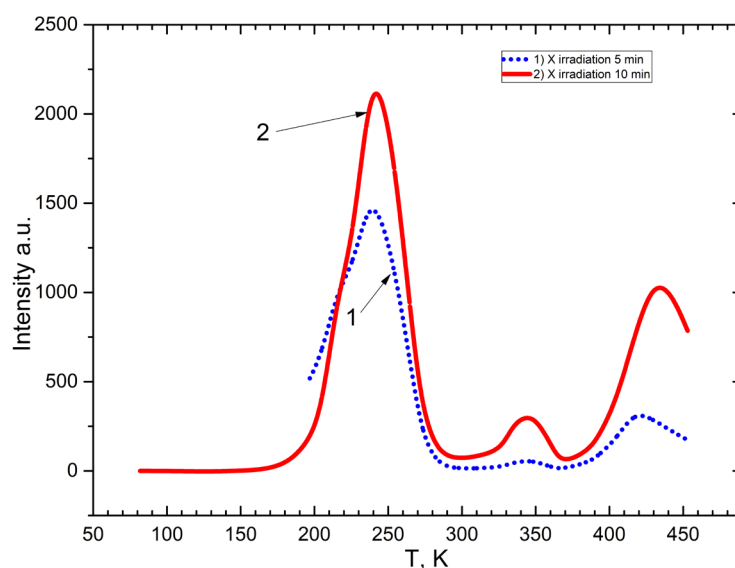


**Figure 9.** TL curve of  $Ca_2P_2O_7 - Mn$  irradiated by X irradiation: 1—5 min; 2—10 min.

In our forthcoming research, we aim to delve into the formation of electron- and hole-trapping centers upon excitation within the vacuum-ultraviolet region, specifically at photon energies ranging from 6.2 eV to 12.4 eV (100–200 nm). This range is critical as it encompasses the energies at which free electron–hole pairs are predominantly formed, particularly above 8 eV (155 nm), as highlighted in the studies by authors [22].

The findings reported by [22] reveal that long-lasting phosphorescence and thermally stimulated luminescence are primarily linked to the creation of electron–hole-trapping centers. These centers emerge through charge transfer from the oxygen anion to the valence band during the excitation of the  $3d$  state of  $Mn^{2+}$  and the  $5d$  states of rare-earth ions, specifically in transitions involving  $O^{2-} - Mn^{2+}$  and  $O^{2-} - Re^{3+}$  complexes. Furthermore, reference [22] correlates the fundamental absorption band observed in matrices such as  $CaBPO_5 - Ce^{3+}$ ,  $LiCaPO_4 - Ce^{3+}$ , and  $Li_2CaSiO_4 - Ce^{3+}$  with electron transitions from the anionic groups  $PO_4^{3-}$  and  $SiO_4^{4-}$  to the conduction band.

In Figure 10, the emission spectrum of the  $\alpha$ - $Ca_2P_2O_7 - Mn$  phosphor, excited by photons at energies of 8.26 eV (150 nm) and 7.75 eV (160 nm), is presented for temperatures of 300 K and 15 K. At 300 K, emissions are observed at 2.06 eV, corresponding to the intracenter emission of the  $Mn^{2+}$  ion (curves 1 and 3). When the temperature is lowered to 15 K, the intensity of the 2.06 eV (600 nm) emission from  $Mn^{2+}$  decreases by a factor of 2 to 2.5, and new emission bands emerge at 2.92 eV (425 nm) and 3.06 eV (405 nm) (curves 2 and 4 in Figure 10). This pattern of emissions is consistent with the observations made under UV irradiation at 6.2 eV (200 nm) photon energy at 77 K. The reduction in the  $Mn^{2+}$  emission band leads to the formation of new electronic trapping centers as a result of the reaction  $Mn^{2+} + e^- \rightarrow Mn^+$ , in conjunction with localized holes in  $(P_2O_7)^{3-}$ , forming  $Mn^+ - (P_2O_7)^{3-}$  complexes.



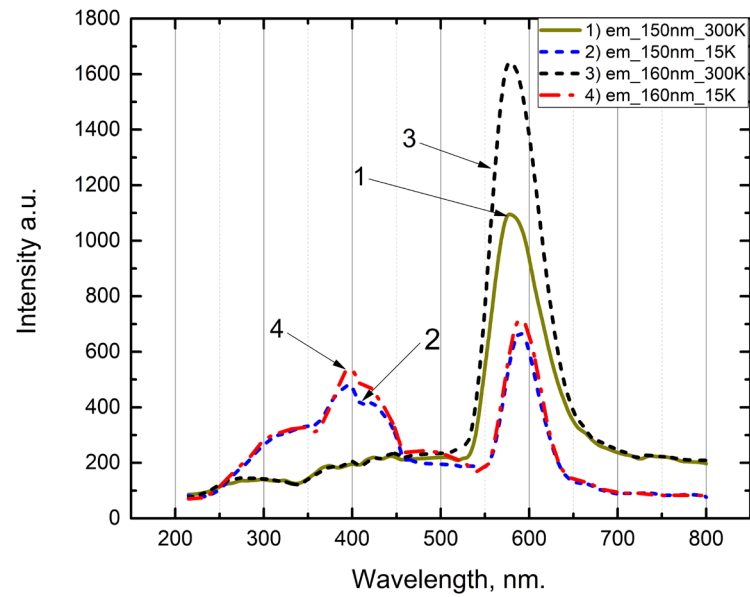


**Figure 10.** Emission spectra of  $\alpha$ - $Ca_2P_2O_7$  phosphor under excitation by photons at 8.26 eV (150 nm) (1—at 300 K, 2—at 15 K) and under excitation by photons at 7.75 eV (160 nm) (3—at 300 K, 4—at 15 K).

Figure 11 shows the excitation spectrum of  $\alpha$ - $Ca_2P_2O_7 - Mn$  emission for the 2.0 eV (620 nm) and 2.1 eV (590 nm) bands at 300 and 15 K. Figure 11 shows that the emission of the  $Mn^{2+}$  ion is excited at photon energies of 7.85 eV (158 nm). This value is the band gap for the phosphor  $\alpha$ - $Ca_2P_2O_7 - Mn$ .

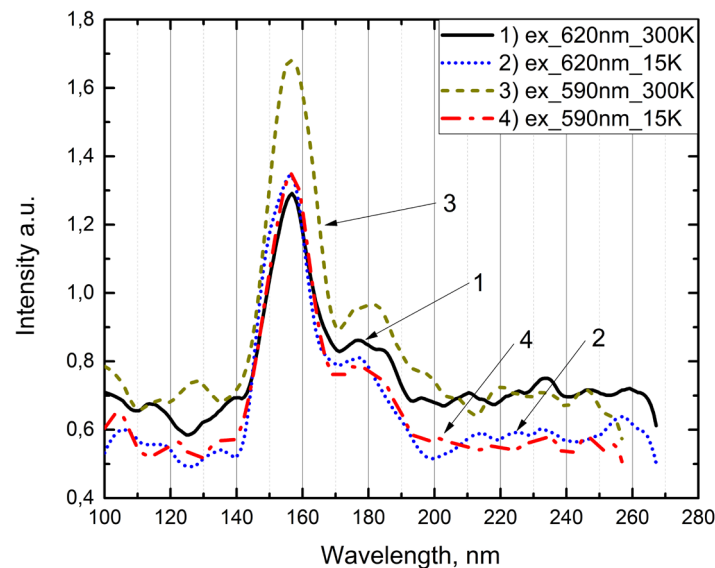


**Figure 11.** Excitation spectra of  $Ca_2P_2O_7 - Mn$  for the emission band at 2.0 eV (620 nm): 1—at 300 K; 2—at 15 K, and for the emission band at 2.1 eV (590 nm): 3—at 300 K; 4—at 15 K.

#### 4. Discussion

The experimental results highlight the following processes occurring in the  $Ca_2P_2O_7 - Mn$  phosphor upon excitation with 6.2 eV (200 nm) ultraviolet photons:

1. The occurrence of impurity intracenter emissions at 2.06 eV (600 nm) from the  $Mn^{2+}$  ion, observable at both 300 K and 77 K.

- The generation of new induced recombination emissions at 2.95 eV (420 nm) and 3.1 eV (405 nm), resulting from charge transfer between excited matrix anions and impurities, specifically between  $(O^{2-} - Mn^{2+})$  and  $O^{2-} - (P_2O_7)^{4-}$ .

To further elucidate the characteristics of the intracenter emission at 600 nm and the newly induced emissions at 2.95 eV (420 nm) and 3.1 eV (405 nm), the excitation spectra of these emissions were meticulously measured.

- Intracenter emission at 2.06 eV (600 nm) are excited:
  - At 3.65 eV (340 nm) and 3.4 eV (335 nm), as shown by the authors of [5], corresponding to intra-center excitations of the  $Mn^{2+}$  ion.
  - At 5.64 eV (220 nm) and 4.96 eV (251 nm) because of charge transfer from the excited anion to impurities and neighboring anions  $(O^{2-} - Mn^{2+})$  and  $O^{2-} - (P_2O_7)^{4-}$ .
  - ~2.5 eV (496 nm) excitation of trap centers near the  $Mn^{2+}$  ion.
  - 4.0 eV (310 nm) and 4.5 eV (275 nm) emissions arising in the transparency region of the  $Ca_2P_2O_7 - Mn$  matrix.
- The newly created induced emissions at 2.95 eV (496 nm) and 3.1 eV (400 nm) are excited at photon energies of 4.0 eV (310 nm) and 4.5 eV (275 nm), as well as in the spectral range of 4.96 eV (256 nm) and 5.64 eV (220 nm), where these new induced emissions are mainly created at low temperatures of 77 K.

Next, to clarify the correlation between the above-mentioned regularities with the processes in the pure matrix  $Ca_2P_2O_7$ , similar experimental studies on the  $Ca_2P_2O_7$  phosphor were conducted.

- When the pure  $Ca_2P_2O_7$  phosphor was excited with photon energies ranging from 5.9 to 6.2 eV (200–210 nm), emissions at 2.95 eV (496 nm) and 3.1 eV (400 nm) were detected at both 77 K and 300 K.
- These induced emissions are excited at photon energies of 4.0 eV (310 nm) and 4.5 eV (275 nm) in the transparency region of the pure  $Ca_2P_2O_7$  matrix and more intensively so at 77 K.

The emission bands for matrix samples of  $Ca_2P_2O_7$  and with an admixture of Mn are listed in Table 1.

**Table 1.** Emission spectra.

Sample	Temperature	Excitation Energy	Emission Peaks	Interpretation
$Ca_2P_2O_7 - Mn$	300 K	6.2 eV (200 nm)	2.06 eV (600 nm), 3.06 eV (405 nm), 2.92 eV (425 nm)	$Mn^{2+}$
	77 K		2.06 eV (600 nm)—low intensity 3.06 eV (405 nm), 2.92 eV (425 nm)—high intensity	$Mn^{2+}$
$Ca_2P_2O_7$	300 K	6.2 eV (200 nm)	2.92 eV (425 nm), 3.06 eV (405 nm),	matrix
		5.64 eV (220 nm)	2.92 eV (425 nm), 3.06 eV (405 nm),	matrix
	77 K	6.2 eV (200 nm)	2.92 eV (425 nm), 3.06 eV (405 nm),	matrix
		5.64 eV (220 nm)	2.92 eV (425 nm), 3.06 eV (405 nm),	matrix

Excitation bands of the type for samples of the matrix and with an admixture of Mn are indicated in Table 2.

Table 2. Excitation spectra.

Sample	Temperature	Emission Peaks	Excitation Energy	Interpretation
$Ca_2P_2O_7 - Mn$	300 K	2.06 eV (600 nm)	4.0–4.5 eV (275–310 nm)	$Mn^{2+}$
	77 K	2.06 eV (600 nm)	2.5 eV (496 nm), 3.0 eV (413 nm), 3.5 eV (354 nm), 4.0 eV (310 nm), 4.5 eV (275 nm), 5.0–6.2 eV (200–248 nm)	$Mn^{2+}$
	300 K	3.06 eV (405 nm), 2.92 eV (425 nm),	3.94–4.0 eV (310–314 nm), 4.5–4.6 eV (269–275 nm), 5.5–6.2 eV (200–225 nm)—weak intensity	matrix
	77 K	3.06 eV (405 nm), 2.92 eV (425 nm),	3.94–4.0 eV (310–314 nm), 4.5–4.6 eV (269–275 nm), 5.5–6.2 eV (200–225 nm)—strong intensity	
$Ca_2P_2O_7$	300 K	2.92 eV (425 nm), 3.06 eV (405 nm),	3.94–4.0 eV (310–314 nm), 4.5–4.6 eV (269–275 nm), 5.64 eV (220 nm).	matrix
	77 K	2.92 eV (425 nm), 3.06 eV (405 nm),	3.94–4.0 eV (310–314 nm), 4.5–4.6 eV (269–275 nm), 5.64 eV (220 nm).	

The main question of these studies is the formation of induced or combined radiative states in pure and doped phosphors in the same manner as a result of charge transfer from the matrix to impurities and neighboring anions ( $O^{2-} - Mn^{2+}$ ) and  $O^{2-} - (P_2O_7)^{4-}$ . As a result, intrinsic and impurity electron-trapping centers  $Mn^+$  and  $(P_2O_7)^{5-}$ , complementary to hole-trapping centers  $(P_2O_7)^{3-}$  near  $Mn^{2+}$  impurities, are formed. During the excitation of the anion  $(P_2O_7)^{4-}$ , due to the charge transfer of  $Mn^{2+}$  impurities,  $Mn^+$  should be created, and the hole component  $(P_2O_7)^{3-}$  is mainly localized near  $Mn^{2+}$  impurities.

It is assumed that similar induced and combined radiative states at 2.95 eV (420 nm) and 3.1 eV (400 nm) should be created upon trapping free electrons and holes by  $Mn^{2+}$  impurities and  $(P_2O_7)^{4-}$  anions. We conducted experimental research in the vacuum ultraviolet spectral range from 12.4 eV (100 nm) to 4.96 eV (250 nm), where free electron-hole pairs are created. When irradiated with photons with energies of 8.26 eV (150 nm) and 7.75 eV (160 nm) at temperatures of 300 K and 15 K, intracenter emissions of  $Mn^{2+}$  at 2.15 eV (577 nm) and new induced or combined radiative states at 2.95 eV (420 nm) and 3.1 eV (400 nm) are created. Impurity emissions of  $Mn^{2+}$  at photon energies of 8.0 eV (155 nm) are excited by free electrons. It is known that the band gap of  $CaBPO_5$  and  $LiCaPO$  phosphors are 8.26 eV (150 nm) and 7.65 eV (162 nm), respectively [22].

The primary focus of these studies is to understand the formation of induced or combined radiative states in both pure and doped phosphors, facilitated by charge transfer from the matrix to impurities and neighboring anions, specifically  $O^{2-} - Mn^{2+}$  and  $O^{2-} - (P_2O_7)^{4-}$ . This process results in the formation of intrinsic and impurity electron-trapping centers ( $Mn^+$  and  $(P_2O_7)^{5-}$ ) that complement hole-trapping centers  $(P_2O_7)^{3-}$  located near  $Mn^{2+}$  impurities. It is proposed that during the excitation of the anion  $(P_2O_7)^{4-}$ , charge transfer from  $Mn^{2+}$  impurities should lead to the creation of  $Mn^+$ , with the hole component  $(P_2O_7)^{3-}$  primarily localized near  $Mn^{2+}$  impurities. Consequently, it is hypothesized that similar induced and combined radiative states at 2.95 eV (420 nm) and 3.1 eV (400 nm) are formed by the trapping of free electrons and holes by  $Mn^{2+}$  impurities and  $(P_2O_7)^{4-}$  anions.

The estimated band gap of  $Ca_2P_2O_7$  is approximately 8.0 eV (155 nm).

Thus, the new combined radiative states are created as a result of charge transfer from the excited ion  $P_2O_7$  to  $Mn^{2+}$  impurities and ions  $(P_2O_7)^{4-}$ .

These radiative states are generated when electrons are captured by impurities and intrinsic centers, specifically through the reactions  $Mn^{2+} + e^- \rightarrow Mn^+$  and  $(P_2O_7)^{4-} + e^- \rightarrow (P_2O_7)^{3-}$ . This results in the formation of impurity  $Mn^+ - (P_2O_7)^{3-}$  and intrinsic  $(P_2O_7)^{5-} - (P_2O_7)^{3-}$  electron-hole-trapping centers. The trapping of electrons by  $Mn^{2+}$

ions and  $(P_2O_7)^{4-}$  anions lead to the creation of these specific centers, facilitating the observed radiative states.

The temperature-dependent measurements of the new radiative states at 2.95 eV (420 nm) and 3.1 eV (400 nm) reveal a distinct pattern: their intensity steadily decreases from 77 K to 250 K, experiences a surge between 250 K and 300 K, and then undergoes a sharp decline from 300 K to 400 K. Concurrently, the intensity of the intracenter emission at 2.06 eV  $Mn^{2+}$  shows a slight decrease over the same temperature range, followed by a significant increase between 370 K and 450 K.

The experimental results, as illustrated in Figures 3, 6 and 8, confirm the temperature dependence of the intensity for the newly induced emissions at 2.95 eV (420 nm) and 3.1 eV (400 nm). Notably, the efficiency of generating these induced emissions at lower temperatures, specifically at 15 K and 77 K, is found to be twice as high compared to that at higher temperatures ranging from 300 K to 350 K.

The observed temperature-dependent behavior of the radiative states at 2.95 eV (420 nm) and 3.1 eV (400 nm), particularly the flaring up and subsequent rapid decrease in intensity between 250 K and 300 K, can be attributed to ionization processes:  $Mn^{+} \rightarrow Mn^{2+} + e^{-}$ ;  $(P_2O_7)^{3-} \rightarrow (P_2O_7)^{4-} + e^{-}$ . This ionization leads to the generation of free electrons in the conduction band, which then recombine with localized holes near the  $Mn^{2+}$  impurity, specifically  $(P_2O_7)^{3-}$ . The energy released during this recombination is transferred to the impurities, resulting in an observed increase in the intensity of intracenter emission at 2.06 eV (600 nm) for  $Mn^{2+}$ . Consequently, this process facilitates energy transfer from the matrix to the impurities. In analogous research conducted by authors [3] on  $KSrPO_4 - Eu^{3+}$ , electron ionization from the  $Eu^{2+}$  ion into the conduction band was observed with an activation energy of 0.4 eV, illustrating a similar charge transfer mechanism.

The decrease in the intensity of the combined radiative state of 2.92 eV (425 nm) and 3.0 eV (413 nm) is associated with the decay of electron-trapping centers and the implementation of electron recombination with a hole-trapping center, which is confirmed by the appearance of TL peaks in this temperature range in the irradiated phosphor  $Ca_2P_2O_7 - Mn$  at 80 K (Figure 9). The presence of TL peaks confirms the formation of electron- and hole-trapping centers during irradiation with UV (6.2 eV (200 nm)) photons.

The formation of induced or combined radiative states, which include the electronic configurations of electron-hole-trapping centers  $Mn^{+} - (P_2O_7)^{3-}$  and  $(P_2O_7)^{5-} - (P_2O_7)^{3-}$ , is supported by experimental evidence. Specifically, new induced emissions at 2.95 eV (420 nm) and 3.1 eV (400 nm), stimulated by the irradiation of trapping centers, are excited at photon energies of 4.0 eV (310 nm) and 4.5 eV (275 nm) within the transparency region of the matrix, as shown in Figures 5 and 6. Similarly, intracenter emissions from the  $Mn^{2+}$  ion are excited at these same photon energies, as demonstrated in Figures 4, 5 and 7.

The experimental evidence solidly supports that induced states arise from the electronic configurations of both intrinsic and impurity-trapping centers. Specifically, the radiative decay and relaxation processes involving the excited state  $Mn^{+} - (P_2O_7)^{3-}$  commence from a singular energy level as the temperature increases. This behavior underscores the dynamic interaction between these trapping centers under thermal variation. Figure 12 presents a model illustrating the presumed arrangement of electronic- and hole-trapping centers, providing a visual representation of these complex interactions.

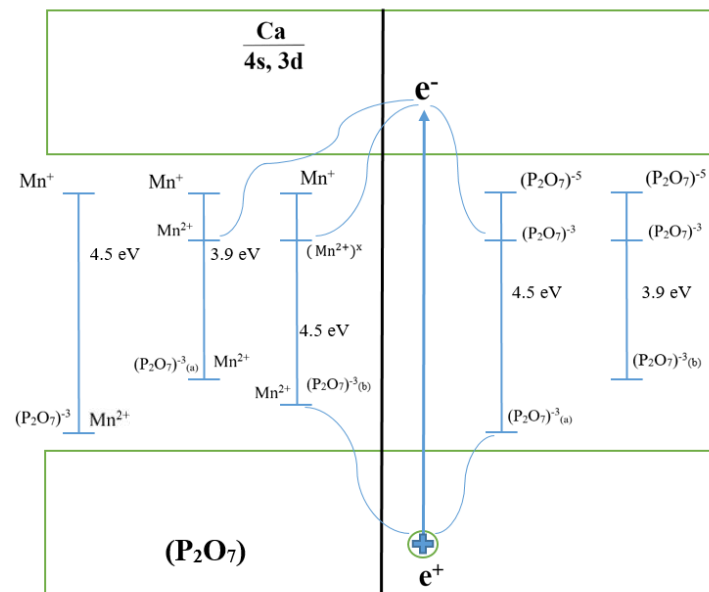


**Figure 12.** Model depicting the arrangement of electronic- and hole-trapping centers.

Here is the explanation of the model describing electronic transitions in irradiated  $Ca_2P_2O_7 - Mn$  at temperatures of 300 K and 77 K.

At a temperature of 300 K, irradiated  $Ca_2P_2O_7$  with photons of 6.2 eV (200 nm) generates electron–hole pairs  $e^+(P_2O_7)^{3-} - e^-$ . Upon the transition from  $6A_1$  to  $4T_1$  in the  $Mn^{2+}$  ion, an emission band occurs at 2.06 eV (600 nm). At temperatures of 77 K and 300 K, a free electron occurs:

Upon capture by  $Mn^{2+}$  impurities:  $Mn^{2+} + e^- \rightarrow Mn^+$ ;

Upon capture by the matrix anions  $(P_2O_7)^{4-} + e^- \rightarrow (P_2O_7)^{5-}$ .

As a result, electronic  $Mn^+$  and hole  $(P_2O_7)^{3-}$  capture centers arise, i.e.,  $Mn^+ - (P_2O_7)^{3-}$ . Hybrid or combined electronic states arise beneath the conduction band consisting of the electronic state  $Mn^+$  and  $(P_2O_7)^{5-}$ .

Parallel to this process, a hole localized above the valence band near the ground state of the  $Mn^{2+}$  ion is localized above the valence band  $(P_2O_7)^{3-}$ . Due to the anisotropic nature of the compound, the holes formed with unpaired electrons in different crystallographic directions localize above the valence band ceiling at different energy positions:  $(P_2O_7)^{3-} (a)$  and  $(P_2O_7)^{3-} (b)$ .

The experimental data obtained by analyzing the photoluminescence decay curves of the samples reveal distinct decay times for different emission bands (Figure 13). Specifically, the decay time for the intracenter emission at 2.06 eV (corresponding to 600 nm or 2 bands) is measured at 55  $\mu s$ . In contrast, the decay time for the induced emission at 3.1 eV (corresponding to 400 nm or 1 band) is significantly shorter at 22  $\mu s$ . The induced photoluminescence from  $Mn^{2+}$  emissions is notably observed following cascade recombination processes, highlighting the complex dynamics of electron–hole recombination in these materials.

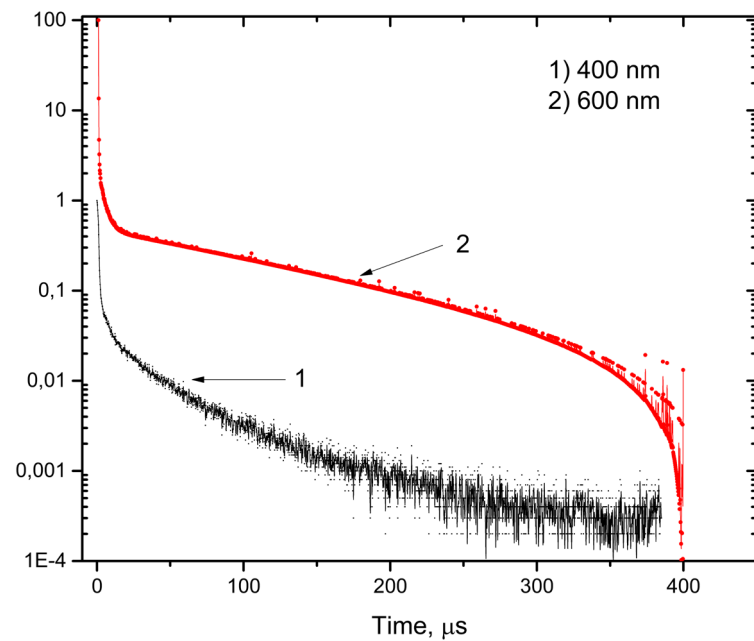


**Figure 13.** Decay curves for emission bands at (1) 3.1 eV (400 nm); (2) 2.06 eV (600 nm).

The photon energies of 4.0 eV (310 nm) and 4.5 eV (275 nm), responsible for exciting the intrinsic and impurity radiative states at 2.95 eV (420 nm) and 3.1 eV (400 nm), correspond to the absorption and excitation energies bridging the ground and excited states of both intrinsic and impurity electron–hole-trapping centers. This relationship is detailed in the band model illustrated in Figure 12. The model elucidates how these specific photon energies facilitate transitions that result in the observed radiative states, providing a comprehensive understanding of the energy dynamics within the phosphor.

## 5. Conclusions

In irradiated  $Ca_2P_2O_7 - Mn$  phosphors, new induced emissions at 2.95 eV (420 nm) and 3.1 eV (400 nm) have been detected, which are excited at photon energies of 4.0 eV (310 nm) and 4.5 eV (275 nm) in the transparency range of the matrix. The new radiative states at 2.95 eV (420 nm) and 3.1 eV (400 nm) are created upon excitation of anions by photons with energies of 5.0 eV (548 nm) and 5.64 eV (220 nm), resulting from charge transfer from the  $(P_2O_7)^{4-}$  ion to the  $Mn^{2+}$  impurities and neighboring ions according to the reaction  $(O^{2-} - Mn^{2+})$  and  $O^{2-} - (P_2O_7)^{4-}$ .

It is shown that the radiative states at 2.95 eV and 3.1 eV are also created upon excitation of anions with photon energies of 8.0 eV and 8.25 eV exceeding the band gap, due to electron-trapping by impurities and neighboring ions according to reactions  $Mn^{2+} + e^- \rightarrow Mn^+$  and  $(P_2O_7)^{4-} + e^- \rightarrow (P_2O_7)^{5-}$ .

Based on the measurement of the excitation spectra of the recombination emission at 2.95 eV (420 nm) and 3.1 eV (400 nm) and the impurity emission at 2.06 eV (600 nm), it has been shown that they are simultaneously excited at photon energies of 4.0 eV (310 nm) and 4.5 eV (275 nm). These values represent the excitation spectrum of the new induced electron radiative states at 2.95 eV (420 nm) and 3.1 eV (400 nm), consisting of intrinsic and impurity electronic trapping center states.

**Author Contributions:** T.N.N.: Supervision, Writing—original draft, Writing—review & editing; T.T.A.: Investigation, Visualization. K.B.Z.: Writing—review & editing, Correspondence; A.S.N.: Investigation, Correspondence; S.P.: Formal analysis, Methodology; D.G.: Investigation; A.Z.: Conceptualization, Methodology; A.K.: Conceptualization, Resources. All authors have read and agreed to the published version of the manuscript.

**Funding:** This research was funded by the Science Committee of The Ministry of Science and Higher Education of the Republic of Kazakhstan (Grant No: AP23488657).

**Data Availability Statement:** Available on request from the authors.

**Conflicts of Interest:** The authors declare no conflict of interest.

## References

1. Cao, R.; Wang, W.; Zhang, J.; Ye, Y.; Chen, T.; Guo, S.; Xiao, F.; Luo, Z. Luminescence properties of Sr<sub>2</sub>Mg<sub>3</sub>P<sub>4</sub>O<sub>15</sub>:Mn<sup>2+</sup> phosphor and the improvement by co-doping Bi<sup>3+</sup>. *Opt. Mater.* **2018**, *79*, 223–226. [[CrossRef](#)]
2. Lecointre, A.; Benhamou, R.A.; Bessi ere, A.; Wallez, G.; Elaatmani, M.; Viana, B. Red long-lasting phosphorescence (LLP) in β-TCP type Ca<sub>9.5</sub>Mn(PO<sub>4</sub>)<sub>7</sub> compounds. *Opt. Mater.* **2011**, *34*, 376–380. [[CrossRef](#)]
3. Zhou, R.; Lin, L.; Liu, C.; Dorenbos, P.; Tao, Y.; Huang, Y.; Liang, H. Insight into Eu redox and Pr<sup>3+</sup> 5d emission in KSrPO<sub>4</sub> by VRBE scheme construction. *Dalton Trans.* **2018**, *47*, 306–313. [[CrossRef](#)] [[PubMed](#)]
4. Griesiute, D.; Garskaite, E.; Antuzevics, A.; Klimavicius, V.; Balevicius, V.; Zarkov, A.; Katelnikovas, A.; Sandberg, D.; Kareiva, A. Synthesis, structural and luminescent properties of Mn-doped calcium pyrophosphate (Ca<sub>2</sub>P<sub>2</sub>O<sub>7</sub>) polymorphs. *Sci. Rep.* **2022**, *12*, 7116. [[CrossRef](#)] [[PubMed](#)]
5. Lecointre, A.; Bessi ere, A.; Bos, A.J.J.; Dorenbos, P.; Viana, B.; Jacquart, S. Designing a red persistent luminescence phosphor: The example of YPO<sub>4</sub>:Pr<sup>3+</sup>,Ln<sup>3+</sup> (Ln = Nd, Er, Ho, Dy). *J. Phys. Chem. C* **2011**, *115*, 4217–4227. [[CrossRef](#)]
6. Zhou, R.; Ma, F.; Su, F.; Ou, Y.; Qi, Z.; Zhang, J.; Huang, Y.; Dorenbos, P.; Liang, H. Site Occupancies, VUV-UV-vis photoluminescence, and X-ray radioluminescence of Eu<sup>2+</sup>-doped RbBaPO<sub>4</sub>. *Inorganic Chemistry. Inorg. Chem.* **2020**, *59*, 17421–17429. [[CrossRef](#)] [[PubMed](#)]
7. Wang, Y.; Brik, M.G.; Dorenbos, P.; Huang, Y.; Tao, Y.; Liang, H. Enhanced green emission of Eu<sup>2+</sup> by energy transfer from the 5D<sub>3</sub> level of Tb<sup>3+</sup> in NaCaPO<sub>4</sub>. *J. Phys. Chem. C* **2014**, *118*, 7002–7009. [[CrossRef](#)]
8. Lecointre, A.; Viana, B.; LeMasne, Q.; Bessi ere, A.; Chan eac, C.; Gourier, D. Red long-lasting luminescence in clinoenstatite. *J. Lumin.* **2009**, *129*, 1527–1530. [[CrossRef](#)]
9. Tang, Q.; Tang, H.; Luo, D.; Zhang, C.; Guo, J.; Wu, H. Thermoluminescence spectra and dose responses of SrSO<sub>4</sub> phosphors doped with rare earths (Eu, Dy, Tm) and phosphorus. *Radiat. Prot. Dosim.* **2019**, *187*, 164–173. [[CrossRef](#)]
10. Song, H.J.; Yim, D.K.; Roh, H.-S.; Cho, I.S.; Kim, S.-J.; Jin, Y.-H.; Shim, H.-W.; Kim, D.-W.; Hong, K.S. RbBaPO<sub>4</sub>:Eu<sup>2+</sup>: A new alternative blue-emitting phosphor for UV-based white light-emitting diodes. *J. Mater. Chem. C* **2013**, *1*, 500–505. [[CrossRef](#)]
11. Zhao, C.; Xia, Z.; Yu, S. Thermally stable luminescence and structure evolution of (K, Rb)BaPO<sub>4</sub>:Eu<sup>2+</sup> solid-solution phosphors. *J. Mater. Chem. C* **2014**, *2*, 6032–6039. [[CrossRef](#)]
12. Hussain, T.; Asfora, V.K.; da Nobrega, B.P.; de Barros, V.S.; de Azevedo, W.M.; Houry, H.J. Thermoluminescence properties of nanocrystalline BaSO<sub>4</sub> doped with Eu<sup>2+</sup> produced by solid state combustion synthesis. *Radiat. Phys. Chem.* **2021**, *186*, 109531. [[CrossRef](#)]
13. Zhai, B.-G.; Liu, D.; He, Y.; Yang, L.; Huang, Y.M. Tuning the photoluminescence of Eu<sup>2+</sup> and Eu<sup>3+</sup> co-doped SrSO<sub>4</sub> through post annealing technique. *J. Lumin.* **2018**, *194*, 485–493. [[CrossRef](#)]
14. Guckan, V.; Altunali, V.; Nur, N.; Depci, T.; Ozdemir, A.; Kurt, K.; Yu, Y.; Yegingil, I.; Yegingil, Z. Studying CaSO<sub>4</sub>:Eu as an OSL phosphor. *Nucl. Instrum. Methods Phys. Res. Sect. B Beam Interact. Mater. At.* **2017**, *407*, 145–154. [[CrossRef](#)]
15. Annalakshmi, O.; Jose, M.T.; Madhusoodanan, U. Synthesis and characterisation of BaSO<sub>4</sub>:Eu thermoluminescence phosphor. *Radiat. Prot. Dosim.* **2012**, *150*, 127–133. [[CrossRef](#)] [[PubMed](#)]
16. Sun, L. Photoluminescence investigation of Eu<sup>2+</sup>-doped BaSO<sub>4</sub>. *Exp. Theor. Nanotechnol.* **2022**, 387–394. [[CrossRef](#)]
17. Adachi, S. Mn<sup>4+</sup> vs Mn<sup>2+</sup>—A comparative study as efficient activator ions in phosphor materials: A review. *J. Lumin.* **2023**, *263*, 119993. [[CrossRef](#)]
18. Adachi, S. Review—Photoluminescence Spectroscopy of Mn<sup>2+</sup>-Activated Phosphors: Part I. Fundamentals. *ECS J. Solid State Sci. Technol.* **2023**, *12*, 126003. [[CrossRef](#)]
19. Adachi, S. Review—Photoluminescence Spectroscopy of Mn<sup>2+</sup>-Activated Phosphors: Part II. Some Representative Phosphors. *ECS J. Solid State Sci. Technol.* **2023**, *12*, 126004. [[CrossRef](#)]
20. Yussupbekova, B.N.; Nurakhmetov, T.N.; Salikhodzha, Z.M.; Zhunusbekov, A.M.; Kainarbay, A.Z.; Daurenbekov, D.H.; Sadykova, B.; Zhangylyssov, K.B. Intrinsic and impurity emission and formation mechanism of trapping centers in LiKSO<sub>4</sub>-Cu crystals. *Nucl. Instrum. Methods Phys. Res. Sect. B Beam Interact. Mater. At.* **2020**, *481*, 19–23. [[CrossRef](#)]
21. Nurakhmetov, T.N.; Alibay, T.T.; Zhangylyssov, K.B.; Daurenbekov, D.H.; Zhunusbekov, A.M.; Kainarbay, A.Z.; Sadykova, B.M.; Tolekov, D.A.; Shamiyeva, R.K. Specific Features of Formation of Electron and Hole Trapping Centers in Irradiated CaSO<sub>4</sub>-Mn and BaSO<sub>4</sub>-Mn. *Crystals* **2023**, *13*, 1054. [[CrossRef](#)]
22. Dorenbos, P.; Pierron, L.; Dinca, L.; Van Eijk, C.W.E.; Kahn-Harari, A.; Viana, B. 4f–5d spectroscopy of Ce<sup>3+</sup> in CaBPO<sub>5</sub>, LiCaPO<sub>4</sub> and Li<sub>2</sub>CaSiO<sub>4</sub>. *J. Phys. Condens. Matter* **2003**, *15*, 511–520. [[CrossRef](#)]

**Disclaimer/Publisher’s Note:** The statements, opinions and data contained in all publications are solely those of the individual author(s) and contributor(s) and not of MDPI and/or the editor(s). MDPI and/or the editor(s) disclaim responsibility for any injury to people or property resulting from any ideas, methods, instructions or products referred to in the content.